Paper

Characterization of an aperture-stacked patch antenna for ultra-wideband wearable radio systems

Maciej Klemm and Gerhard Troester

Abstract— This paper presents, for the first time, the time-domain characteristics of an aperture-stacked patch antenna (ASPA) for ultra-wideband (UWB) wearable devices. The methodology of antennas characterization for UWB radio systems is also outlined. The antenna operates within the 3–6 GHz frequency band. Time- and frequency-domain characteristics of this antenna are presented in transmission mode (Tx), receiving mode (Rx) and for 2-antenna (Tx-Rx) system. The pulse driving the antenna has duration of 0.65 ns. In the Tx mode, pulses radiated in different directions of the H-plane have very similar shapes. Fidelity factors are as high as 91.6–99.9%. For 2-antenna system, pulses received in normal and end-fire-like directions have the fidelity of 69.5%. As it was found, antenna does not behave "reciprocal" comparing Tx and Rx modes. For normal propagation direction, radiated pulse is the 2nd derivative of the input waveform, but in the Rx mode, received pulse is the 1st derivative of the incident plane wave. This antenna can be used for transmission of short-pulses, even 0.65–1 ns in duration. It is also small (patch planar dimensions 32/19 mm) and compact. Microstrip configuration allows further integration of active devices on the same board. Taking into account above results we can say that ASPA is a good candidate for UWB non-invasive wireless body area network (WBAN) applications.

Keywords— ultra-wideband, UWB, ultra-wideband antennas, ultra-wideband communication.

1. Introduction

Ultra-wideband (UWB) communication systems have recently received more and more attention in the wireless world. Their envisioned advantages over conventional wireless communication systems are: extremely low power consumption, high data rates and simple hardware configuration. UWB radio is characterized by a wide signal spectrum and low radiated power spectral density (for FCC regulation refer to [2]). The most interesting approach of the UWB radio system is so-called **impulse radio** [3]. Its basic concept is to transmit and receive very short electromagnetic pulses (few tens of picoseconds to few nanoseconds in duration), where the pulse shape is a crucial information. Antennas play a critical role in UWB communication systems since they influence the complexity of the receiver and transmitter (pulse generator). Generally, ordinary wideband antennas will not transmit short pulses without distortions. Good examples are well-known broadband radiators: log-periodic and spiral antennas. They can be called ultra-wideband in terms of the input matching and radiation characteristics, but since they radiate different frequency components from different parts of the antenna, fast transient waveforms are distorted and stretched out [4, 5]. Other radiators (e.g., bow-ties or dipoles) use resistive loading to improve transient characteristics, but at the cost of the radiation efficiency.

Design of the ultra-wideband antenna for UWB wearable devices is even more challenging. The antenna is mounted on the human body and more aspects are of great importance: antenna dimensions, possibilities of integration into the clothing, human body influence on the antenna characteristics and also on the short-pulses propagation.

Our research interests concern antennas for non-invasive wireless body area networks (WBAN) [1]. WBAN nodes are usually placed close to the body, on or in everyday clothing. It has some distinct features from other wireless networks, which are also constraints for antenna designs: close proximity of the human body (electromagnetic "pollution" should be extremely low), low transmitting power, possibly low radiation towards body. From the practical point of view, aperture-stacked patch microstrip antenna is a very attractive candidate for WBAN applications (is small and compact, do not radiate significant power into the human body). Moreover, its wideband matching and radiation characteristics were reported [6]. To make sure that ASPA is suitable for UWB (pulsed) WBAN wearable radios, we have investigated its transient characteristic.

2. Antennas in UWB systems

Characteristic parameters of antennas for UWB communication differ from those known from the classical antenna theory. The classic concepts of return loss, gain, and radiation pattern are not applicable to pulsed antennas. Return loss still can be useful in guiding the efficiency, but is no longer a useful measure to characterize short-pulse radiation. Typical antenna parameters for UWB radio systems are described in [7, 8].

Figure 1 schematically presents components of a UWB radio link, which can be equally characterised in the time- or frequency-domain. $X(f)$ represents the signal created in the pulse generator, which feeds the transmit (Tx) antenna. Next, we have 3 transfer functions: $H_{tx}(f)$ stands for the Tx antenna transfer function, $h_{ch}(t)$ indicates channel

characteristics, $H_{rx}(f)$ is the receiving (Rx) antenna transfer function. All these functions are not only time (frequency) dependent, but depend also on the direction of the signal propagation.

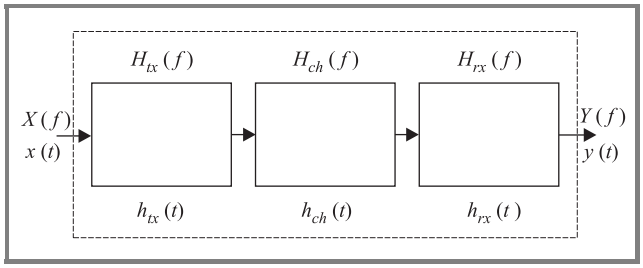

Fig. 1. Schematic of the UWB communication link.

The characteristic feature in the UWB radio systems is that an antenna must be designed taking into account the entire system. For the particular waveform driving different antennas, in the receiver we will get different pulse shapes. Thus, depending on the receiving method, the system performance will vary and in the worst case it can even stop working. This can be the case for the template receiver (e.g., Rake), where the received waveform in compared with the reference pulse. For this kind of receiver, its complexity will depend on the excitation pulse and the antennas

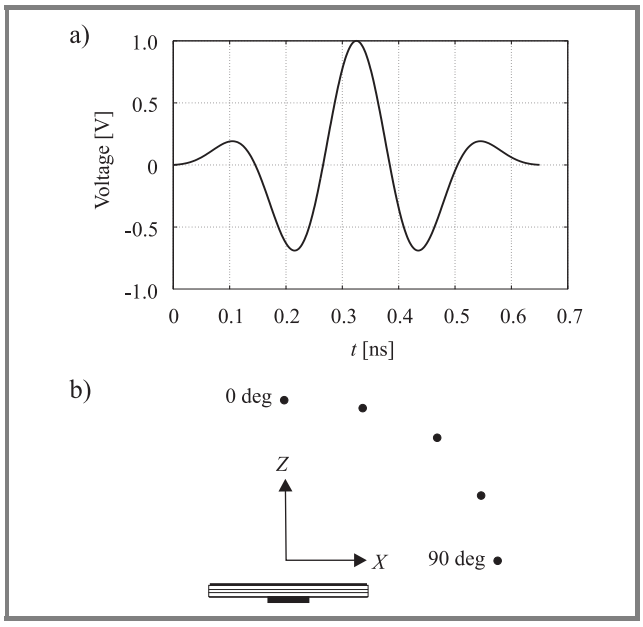

Fig. 2. (a) Excitation pulse driving the antenna; (b) time-domain electric field probes.

used. From the other side, for the same kind of the template receiver, one could assume different approach. To achieve the simplest detection, one can define the received pulse shape $y(t)$, and based on the known function $h(t)$, one could calculate desired excitation $x(t)$. So, in this case we could achieve the simple receiver, but since $x(t)$ can be the arbitrary waveform, pulse generation can become quite complicated. For our investigations we have used the pulse, which comprise trade-off between transmitter and receiver complexities.

Figure 2 presents the excitation pulse (with duration of 0.65 ns and time-domain probes, 20 cm from antenna) used within simulations to find Tx transfer functions for different directions. The pulse was created by the method described in [9]. In this method, for a given duration of the pulse and a limited signal bandwidth we get the set of orthogonal pulses.

3. Antenna design

The geometry of the aperture-stacked patch microstrip antenna is shown in Fig. 3. It differs from typical aper-

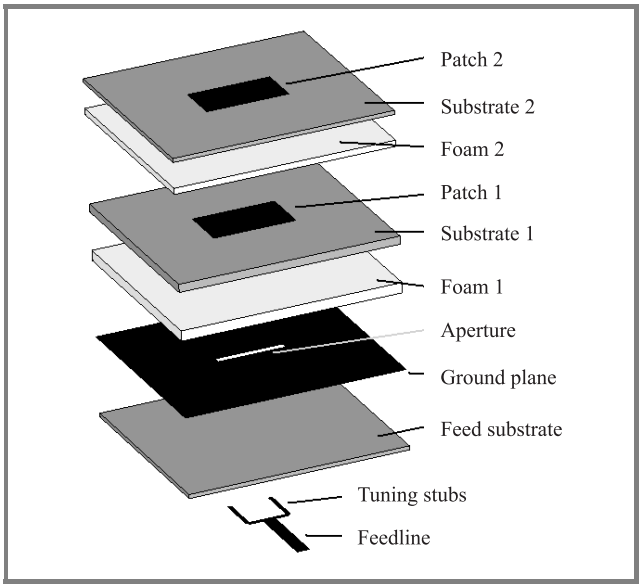

Fig. 3. Geometry of an aperture-stacked patch antenna.

Table 1
Dimensions of the ASPA and materials

Element	h [mm]	ε_r	tan δ
Feed substrate	1.58	2.2	0.0009
Foam substr. 1	4	1.07	0.0009
Substrate 1	3.175	2.2	0.0009
Foam substr. 2	2.4	1.07	0.0009
Substrate 2	1.58	2.2	0.0009
	width [mm]	length [mm]	
Feed-line	4.8	–	
Stubs	1.4	7.4*	
Patch 1	32	19	
Patch 2	32	17	

* Distance from the open-end of a stub to the aperture centre.

ture-coupled patch antennas in that a larger aperture and thicker substrates with low dielectric constants have to be used. Because the aperture in the ASPA is also used as a radiator, dual-offset tuning stubs control the coupling from the feed-line. Length and distance between them are one of the important parameters to achieve broadband characteristics. For our application, we have designed the ASPA for a frequency range from 3 to 6 GHz, considering the input matching. Referring to the antenna geometry from Fig. 3, the antenna dimensions are shown in Table 1.

4. Antenna characteristics

The antenna was designed and analysed with the aid of the commercial time-domain simulator CST microwave studio (finite integration (FI) method). All the necessary frequency domain parameters were calculated applying the Fourier transformation.

4.1. Frequency domain (FD) characteristics

The measured and simulated return losses (RL) of the ASPA (with a ground plane size of 70×70 mm) are shown in Fig. 4. The RL 10 dB bandwidth is from around 3 to 6 GHz, what is sufficient for our application. A small difference between both RL characteristics is a result of the additional SMA connector used in the measurements.

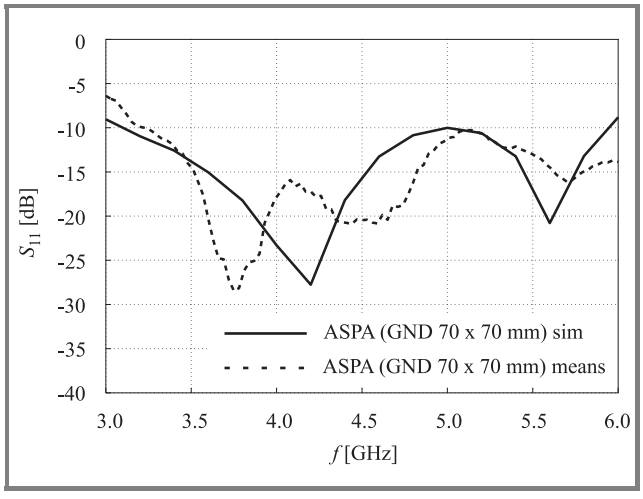

Fig. 4. Measured and simulated input matching of the ASPA.

The $H_{tx}(f)$ transfer function in different radiation directions (see Fig. 2b) is shown in Fig. 5. The 0 deg indicates radiation perpendicular to the patch surface (normal mode), 90 deg is for end-fire-like propagation (what can represent, e.g., communication between antennas placed along the human body). Since the antenna has the linear polarisation, all results are shown for a dominant electric field component. The distance from the antenna to electric field probes is 20 cm.

From Fig. 5a we can see that the transfer function is flat (max. variations 3 dB) within 3–6 GHz bandwidth, for 0–45 deg directions. Together with linear phase for these

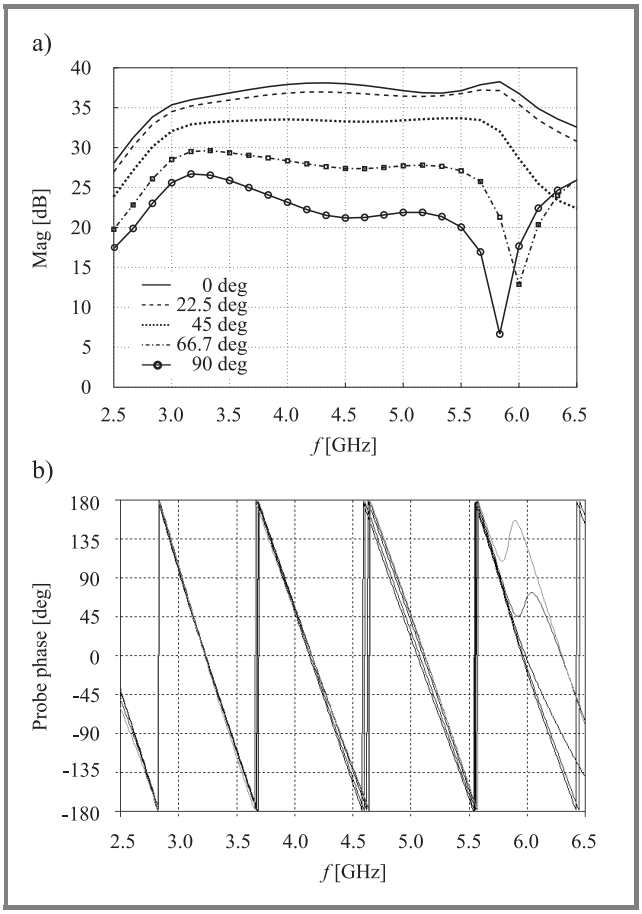

Fig. 5. Antenna FD transfer function $H_{tx}(f)$ in different propagation directions: (a) amplitude; (b) phase.

directions (Fig. 5b) this indicates that the pulse components in this range are radiated without distortions. For radiation at angles between 66.7 and 90 deg, we can see a notch (6 and 5.8 GHz) in the amplitude characteristic of the $H_{tx}(f)$, which causes also nonlinear phase response. The same effect can be seen in Fig. 6, where we have $H_{rx}(f)$ and $H(f)$ (2-antenna) transfer functions. This result probably from the slot radiation. For these directions on the frequencies where the notch occurs, waves radiated from 2 slot edges have aprox. 180 deg phase difference. For the worst case, end-fire-like (90 deg) propagation direction, variations in the amplitude of $H_{tx}(f)$, $H_{rx}(f)$ and $H(f)$ (for 3–6 GHz range) are 20, 30 and 47 dB, respectively. This suggests that the pulse will suffer from distortions. For 0 deg direction, these variations are very small, not higher than 4 dB for all transfer functions ($H_{tx}(f)$, $H_{rx}(f)$ and $H(f)$). Interesting to notice is the fact that $H_{tx}(f)$

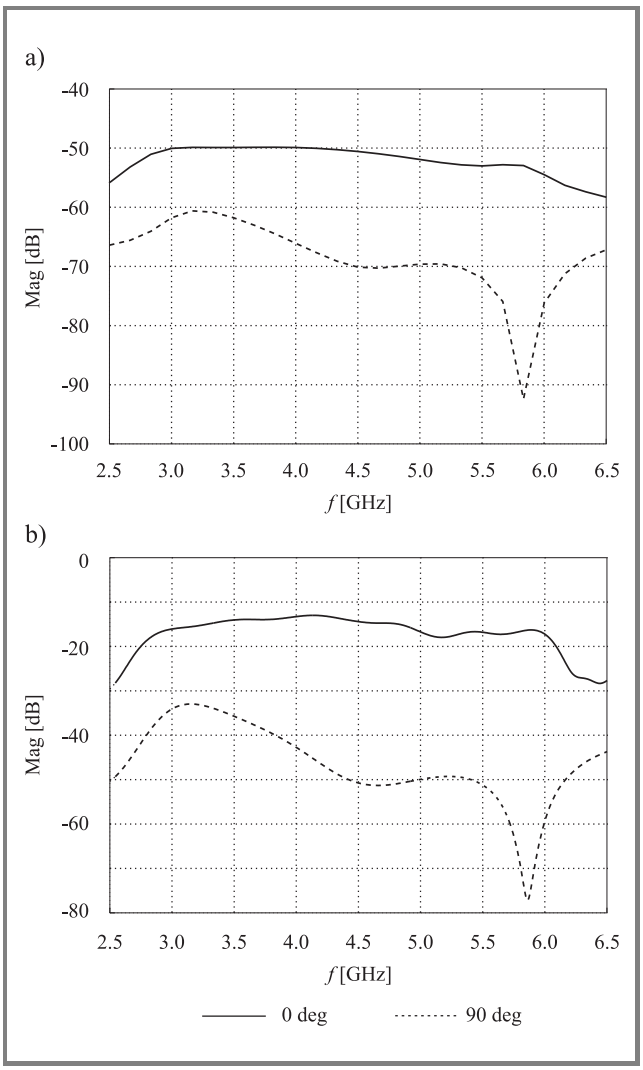

Fig. 6. ASPA transfer functions: (a) $H_{rx}(f)$ – Rx mode; (b) $H(f)$ – 2-antenna system.

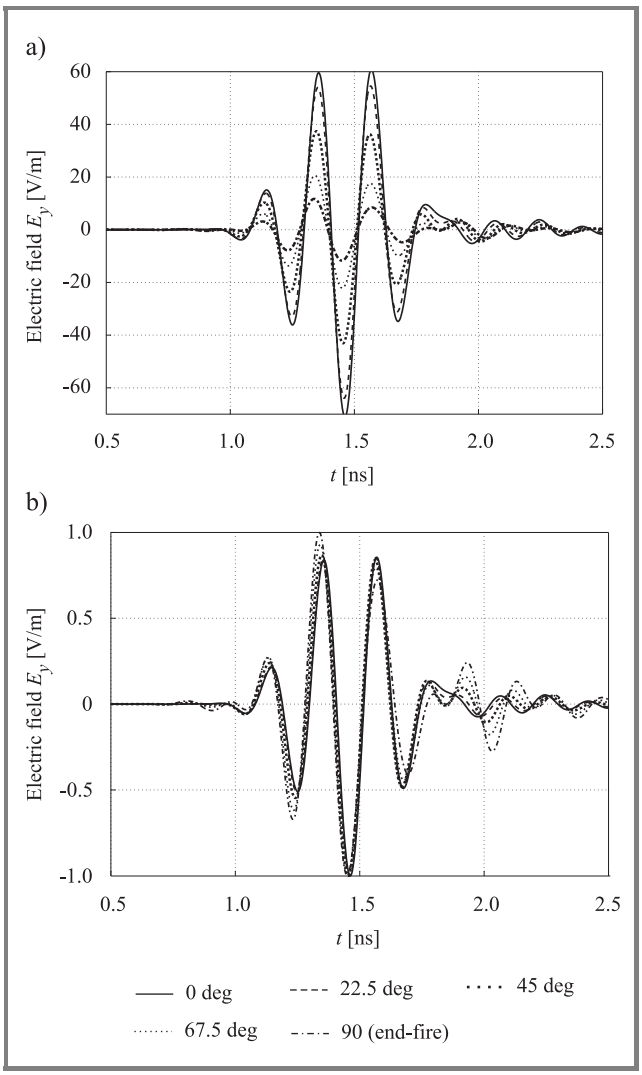

Fig. 7. Radiated pulses (Tx mode): (a) absolute values; (b) normalised values.

and $H_{rx}(f)$ functions are not the same, thus indicating differences in the antenna transmission and reception behaviours. As we will see in the next paragraph this fact has great influence on the pulse shapes.

4.2. Time domain (TD) characteristics

In Fig. 7 we present radiated pulses in five different directions, when the ASPA was excited by the pulse from Fig. 3a. Figure 7 shows absolute and normalized (to the maximum) values of electric field intensity of radiated pulses, respectively. From Fig. 7b we can see the fidelity (pulse shape changes in different propagation directions) of the pulses. Assuming as a reference pulse radiated in a normal direction, the fidelities are 99.9, 99.2, 97 and 91.6% for directions 22.5,45, 66.7 and 90 deg, respectively.

All pulses are very similar, nevertheless for 66.7–90 deg directions we can see the late-time ringing, caused by the notch and nonlinear phase of the Tx transfer function ($H_{tx}(f)$). To avoid pulse distortions, antenna for UWB systems should have the linear phase response. This is even better visible when looking at the pulse shapes (normalized) at the terminals of the receiving antenna (we used the same ASPA in Tx and Rx modes) from Fig. 8. They differ not only in the shape, but also in the duration. Their fidelity is only 69.5%, their duration (counted for the 10% of a V_{max}) is 0.89 and 1.62 ns, for normal and end-fire-like directions, respectively. The longer pulse duration for 90 deg indicates lower achievable data-rates; its complicated shape (more zero-crossing points within the effective duration of the pulse) can make the detection process more difficult (e.g., more fingers for the Rake receiver).

In the UWB transmitter-receiver system, output signals can be (with some assumptions) often approximated by several time derivatives of the input driving pulse (e.g., output waveform from the 2 electrically small Tx-Rx dipoles is a 3rd derivative of the input pulse) [10, 11]. But if the antennas are not electrically small (e.g., horn or reflector antennas) they can have no influence on the pulse shape.

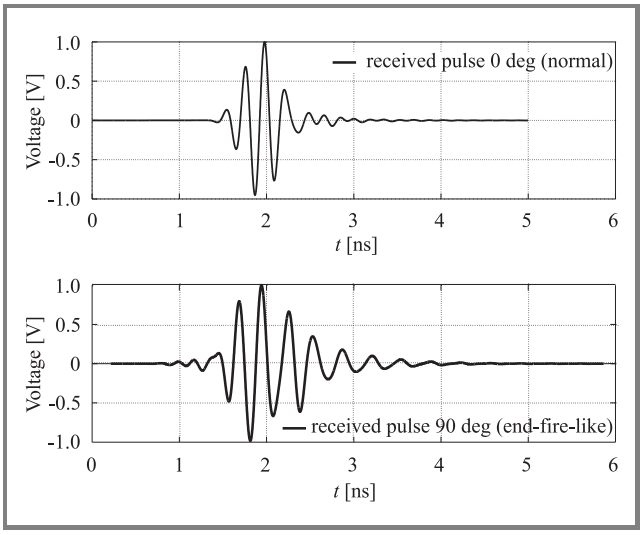

Fig. 8. Received pulses (the same ASPA used for Tx and Rx).

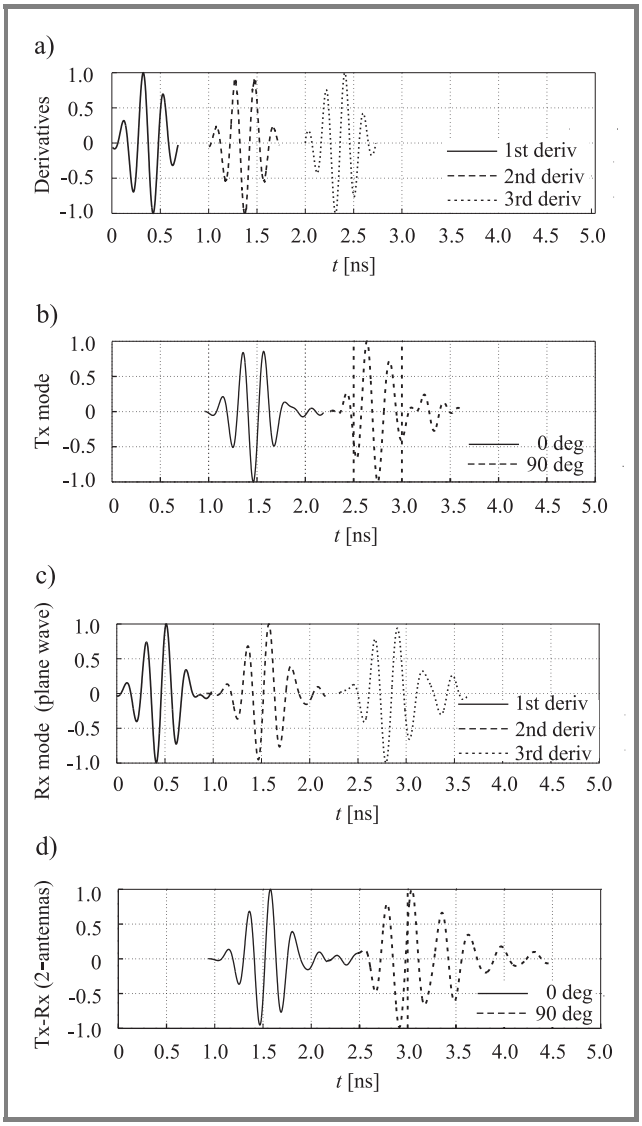

Fig. 9. Comparison between ideal derivatives of the antenna input waveform (Fig. 2a) and its output signal for different operating modes: (a) derivatives of the input pulse; (b) Tx mode; (c) Rx mode; (d) Tx-Rx mode (2 antennas).

Other behaviours, even integrations, are also possible. For that reason we have also investigated this aspect. Figure 9 presents comparison between ideal derivatives of input signal for Tx, Rx (input signal as a plane wave) and Tx-Rx modes. All pulses are normalised so that we can compare their shapes.

In Fig. 9a we have waveforms of the 1st, 2nd, 3rd derivative of the input pulse (Fig. 3a). Figure 9b presents radiated waveforms for 0 and 90 deg directions (the same as in Fig. 7). It can be seen that the pulse radiated in 0 deg direction is very similar to the 2nd derivative of the excitation. For 90 deg direction, excluding late-time distortions, the pulse is a good replica of the 1st derivative of the input waveform. This effect is very interesting, especially if we compare it with the results obtained for the Rx mode. In Rx mode, we have used plane wave excitation with the time shape as for the radiated pulse (Fig. 9b, left) in normal direction (0 deg). The left pulse in Fig. 9c is the 1st derivative of the plane wave pulse, next to it we see 2 received pulses. Unlike in the Tx mode, both pulses are very similar to the 1st derivative of the impinging plane wave. For 90 deg direction, pulse is stretched and distorted at the end, because of the notch in the Rx transfer function. These results show that the antenna is not "reciprocal" in Tx and Rx modes, if we look at the output waveforms (or frequency dependence of the respective transfer functions). Finally, for the entire Tx-Rx system, we can notice that: for 0 deg direction, the received pulse is the replica of the 3rd derivative of the input waveform; for 90 deg direction, the pulse is seriously distorted and stretched in time, and there is no simple relation with any of derivatives. This is the effect of the total system transfer function characteristic $H(f)$ (Fig. 6b, 90 deg). From Fig. 9 we can also say that the reception mechanism has the bigger influence of the pulse distortions, in the end-fire-like transmission direction.

5. Conclusions

In this paper we investigated the ASP microstrip antenna for UWB wearable applications. Based on the general methodology (using TD simulator), the most important parameters of the pulse antenna were found. Their knowledge is necessary to perform simulations of the UWB radio system, including pulse generator, UWB channel model and receiver front-end. It is very difficult to judge the pulse antenna performance, since it cannot be separated from the entire system. There is a clear call for the generator-antenna-receiver co-design in UWB radios. Because of the high fidelity of radiated pulses (above 90%), ASPA could be successfully used for transmitting-only nodes of the WBAN, in the case of on-the-body and body-environment communications scenarios. But it could also be used in both (Tx and Rx) modes, if we could

accept lower data-rates for end-fire-like direction (which is the case for on-the-body placed network nodes). In this case, the template receiver is probably not the best solution. Taking into account all practical requirements (small size and compactness), we can say that ASPA is a good candidate for UWB wearable radio systems. Further investigations will include influence of the human body on the antenna parameters and UWB signals propagation.

References

[1] T. Zasowski, F. Althaus, M. Stäger, A. Wittneben, and G. Tröster, "UWB for noninvasive wireless body area networks: channel measurements and results", in *IEEE Conf. Ultra-Wideband Syst. Technol.*, Reston, USA, 2003.

[2] Federal Communication Commission, "First Order and Report, revision of Part 15 of the Commissions Rules Regarding UWB Transmission Systems", FCC 02-48, Apr. 2002.

[3] M. Z. Win and R. A. Scholtz, "Impulse radio: how it works", *IEEE Commun. Lett.*, vol. 2, issue 2, pp. 36–38, 1998.

[4] W. Soergel, Ch. Waldschmidt, and W. Wiesbeck, "Antenna characterisation for ultra wideband communications", in *2003 Int. Works. Ultra Wideband Syst. IWUWBS*, Oulu, Finland, 2003.

[5] E. K. Miller and J. A. Landt, "Short-pulse characteristics of the conical spiral antenna", *IEEE Trans. Anten. Propagat.*, vol. 25, no. 5, 1977.

[6] S. D. Targonski, R. B. Waterhouse, and D. M. Pozar, "Design of wide-band aperture-stacked patch microstrip antennas", *IEEE Trans. Anten. Propagat.*, vol. 46, no. 9, 1998.

[7] Ch. Robin, S. Bories, and A. Sibille, "Characterisation tools of antennas in the time domain", in *2003 Int. Works. Ultra Wideband Syst. IWUWBS*, Oulu, Finland, 2003.

[8] A. Shlivinski, E. Heyman, and R. Kastner, "Antenna characterisation in the time domain", *IEEE Trans. Anten. Propagat.*, vol. 45, no. 7, 1997.

[9] B. Parr, B. Cho, K. Wallace, and Z. Ding, "A novel ultra-wideband pulse design algorithm", *IEEE Commun. Lett.*, vol. 7, no. 5, 2003.

[10] R. W. Ziolkowski, "Properties of electromagnetic beams generated by ultra-wide bandwidth pulse-driven arrays", *IEEE Trans. Anten. Propagat.*, vol. 40, no. 8, 1992.

[11] C. E. Baum, "General properties of antennas", *IEEE Trans. Electromag. Compat.*, vol. 44, no. 1, 2002.

Maciej Klemm was born in Kwidzyn, Poland, on September 7, 1978. He received the M.S.E.E. degree in microwave engineering from Gdańsk University of Technology, Gdańsk, Poland, in 2002. He is currently working toward his Ph.D. degree in electrical engineering at the Electronics Laboratory of the Swiss Institute of Technology in Zurich, Switzerland. His current research interests include microwave and millimetre-wave circuits design, ultra-wideband antennas, UWB communication systems, MCM technologies, computational electromagnetic methods and simulations.
e-mail: klemm@ife.ee.ethz.ch
Electronics Laboratory
ETH Zurich
Gloriastrasse 35
CH-8092 Zurich, Switzerland

Gerhard Troester received the M.Sc. degree from the Technical University Karlsruhe, Germany, in 1978 and the Ph.D. degree from the Technical University of Darmstadt, Germany, in 1984, both in electrical engineering. He is a Professor and head of the Electronics Laboratory, ETH Zurich, Switzerland. During the eight years he spent at Telefunken Corporation, Germany, he was responsible for various national and international research projects focused on key components for ISDN and digital mobile phones. His field of research includes wearable computing, reconfigurable systems, signal processing, mechatronics, and electronic packaging. He authored and co-authored more than 100 articles and holds five patents. In 1997, he co-founded the spinoff u-blox ag.
e-mail: troester@ife.ee.ethz.ch
Electronics Laboratory
ETH Zurich
Gloriastrasse 35
CH-8092 Zurich, Switzerland